Development 139, 2308-2320 (2012) doi:10.1242/dev.075861

Neurogenin 2 regulates progenitor cell-cycle progression and Purkinje cell dendritogenesis in cerebellar development

Marta Florio[1,*], Ketty Leto[2], Luca Muzio[1], Andrea Tinterri[1,3], Aurora Badaloni[1], Laura Croci[1], Paola Zordan[1], Valeria Barili[1], Ilaria Albieri[1], François Guillemot[4], Ferdinando Rossi[2,‡] and G. Giacomo Consalez[1,‡]

SUMMARY

By serving as the sole output of the cerebellar cortex, integrating a myriad of afferent stimuli, Purkinje cells (PCs) constitute the principal neuron in cerebellar circuits. Several neurodegenerative cerebellar ataxias feature a selective cell-autonomous loss of PCs, warranting the development of regenerative strategies. To date, very little is known as to the regulatory cascades controlling PC development. During central nervous system development, the proneural gene neurogenin 2 (*Neurog2*) contributes to many distinct neuronal types by specifying their fate and/or dictating development of their morphological features. By analyzing a mouse knock-in line expressing Cre recombinase under the control of *Neurog2* cis-acting sequences we show that, in the cerebellar primordium, *Neurog2* is expressed by cycling progenitors cell-autonomously fated to become PCs, even when transplanted heterochronically. During cerebellar development, *Neurog2* is expressed in G1 phase by progenitors poised to exit the cell cycle. We demonstrate that, in the absence of *Neurog2*, both cell-cycle progression and neuronal output are significantly affected, leading to an overall reduction of the mature cerebellar volume. Although PC fate identity is correctly specified, the maturation of their dendritic arbor is severely affected in the absence of *Neurog2*, as null PCs develop stunted and poorly branched dendrites, a defect evident from the early stages of dendritogenesis. Thus, *Neurog2* represents a key regulator of PC development and maturation.

KEY WORDS: Neurog2, Ngn2, Purkinje cells, Cell cycle, Cerebellum, Dendrite

INTRODUCTION

Cerebellar neurogenesis is compartmentalized, with progenitors located in the cerebellar ventricular zone (cbVZ) giving rise to all GABAergic neurons, including Purkinje cells (PCs), and rhombic lip (RL) precursors producing glutamatergic neurons, including granule cells (GCs) (Carletti and Rossi, 2008). The mechanisms by which diverse GABAergic populations diverge from their common progenitors are still unclear. All GABAergic cell types in the cbVZ share lineage relationships (Mathis and Nicolas, 2003) and require pancreatic transcription factor 1a (Ptf1a) (Sellick et al., 2004; Hoshino et al., 2005; Pascual et al., 2007). In the mouse, a population of $Pax2^+$ progenitors appears in the cbVZ around embryonic day (E) 12 and spreads into the prospective white matter (Maricich and Herrup, 1999). All cerebellar inhibitory interneurons derive between E12 and postnatal day (P) 15 from those $Pax2^+$ precursors, and their subtype specification is entirely dependent on environmental cues (Leto et al., 2006; Glassmann et al., 2009; Leto et al., 2009).

Unlike GABAergic interneurons, PCs are born between E11 and E13 as their progenitors exit the cell cycle and start to leave the cbVZ, migrating to the cortex, forming the PC plate, and projecting an axon and an intricate dendritic arbor (reviewed by Sotelo and Rossi, 2011). The regulatory cascades that preside over PC fate specification and maturation are only partially dissected. Further work is required to identify the factors that regulate PC fate choice, cell-cycle progression and exit, differentiation (Zhao et al., 2007), migration (Goldowitz et al., 1997; Rice et al., 1998; Trommsdorff et al., 1999; Park and Curran, 2008), survival (e.g. Croci et al., 2006; Croci et al., 2011), axonogenesis (Sillitoe et al., 2009; Miyata et al., 2010) and dendritogenesis (Boukhtouche et al., 2006; Poulain et al., 2008).

Proneural genes play a pivotal role in neuronal development, triggering a generic neuronal differentiation program and contributing to the specification of distinct neuronal phenotypes throughout the central nervous system (CNS) (reviewed by Bertrand et al., 2002; Ross et al., 2003). Three proneural genes are expressed in the cbVZ (Zordan et al., 2008; reviewed by Consalez et al., 2011), namely *Ascl1* (*Mash1*), *Neurog1* (*Ngn1*) and *Neurog2* (*Ngn2*), and represent suitable candidate regulators of PC development. They are expressed in partially overlapping domains in the $Ptf1a^+$ cbVZ, possibly contributing to its regionalization. $Ascl1^+$ progenitors contribute to PCs and GABAergic interneurons. *Ascl1* null mice lose all GABAergic cerebellar interneurons, whereas PCs are unaffected (Kim et al., 2008; Grimaldi et al., 2009; Sudarov et al., 2011). $Neurog1^+$ progenitors give rise to inhibitory cortical interneurons and to some PCs (Kim et al., 2008; Lundell et al., 2009). However, nothing is known regarding the fate of $Neurog2^+$ progenitors or the role(s) played by *Neurog2* in cerebellar neurogenesis. *Neurog2* is a direct downstream target of the Ptf1a-Rbpj transcription complex (Henke et al., 2009).

In the present work, through a combination of genetic inducible fate mapping (Joyner and Zervas, 2006), targeted deletion and overexpression, we: (1) illustrate the roles played by *Neurog2* in regulating cell-cycle progression and neuronal output in the

[1]Division of Neuroscience, San Raffaele Scientific Institute, 20132 Milan, Italy. [2]Neuroscience Institute of the Cavalieri-Ottolenghi Foundation and Neuroscience Institute of Turin, Department of Neuroscience, Section of Physiology, University of Turin, 10043 Turin, Italy. [3]Università Vita-Salute San Raffaele, 20132 Milan, Italy. [4]Division of Molecular Neurobiology, National Institute for Medical Research, Mill Hill, London NW7 1AA, UK.

*Present address: Max Planck Institute of Molecular Cell Biology and Genetics, 01307 Dresden, Germany
‡Authors for correspondence (ferdinando.rossi@unito.it; g.consalez@hsr.it)

Accepted 18 April 2012

cerebellar VZ; (2) identify the cerebellar lineages, primarily PCs, that originate from *Neurog2*$^{+}$ progenitors; and (3) describe the non-redundant function played by *Neurog2* in the context of PC dendritogenesis.

MATERIALS AND METHODS

Animals and surgical procedures

The experimental plan was designed in agreement with the stipulations of the San Raffaele Institutional Animal Care and Use Committee. Surgical procedures were performed on mice anesthetized with Avertin (Sigma, St Louis, MO, USA).

Generation of *Neurog2::ERT2iCreERT2* knock-in mice

A BAC clone spanning the mouse *Neurog2* locus was modified by homologous recombination in *E. coli* (Copeland et al., 2001) by inserting the ERT2iCreERT2 construct (Casanova et al., 2002) into exon 2, replacing the entire *Neurog2* coding sequence. A plasmid was generated from the recombinant BAC clone by gap repair (Liu et al., 2003) and used to electroporate mouse embryonic stem (ES) cells (strain V6.4). Homologous recombinant ES clones were identified by Southern blotting and injected into C57BL/6 blastocysts that were transferred to CD1 pseudopregnant females.

Mouse genetics

All experiments were conducted on congenic embryos (generation N_8) obtained by backcrossing heterozygotes into the C57BL/6 strain. *Neurog2*$^{CreER/+}$ knock-in mice were crossed with *Rosa26*$^{lacZ/lacZ}$ (Soriano, 1999) or *Rosa26*$^{YFP/YFP}$ (Srinivas et al., 2001) mice. Because null mutants on the C57BL/6 background die around birth (Fode et al., 1998), postnatal stages were analyzed in F2 mutants obtained by outcrossing C57BL/6 heterozygotes with outbred CD1 mice, then intercrossing the F1 progeny. Four percent of null mutants survived past P15.

In situ hybridization

Digoxygenin-labeled riboprobes were transcribed from linearized *Neurog2* and *CreER* plasmids. Hybridizations were performed as described (Croci et al., 2006).

Deoxyuridine labeling

Pregnant dams were injected intraperitoneally (i.p.) (50 μg/g body weight) with the following synthetic thymidine analogs: 5-bromo-2-deoxyuridine (BrdU; Sigma), 5-chloro-2-deoxyuridine (CldU; Sigma), 5-iodo-2-deoxyuridine (IdU; Sigma) and 5-ethynyl-2′-deoxyuridine (Edu; Invitrogen, Carlsbad, CA, USA). For cumulative EdU labeling, timed females were injected i.p. every 3 hours for up to 18 hours. BrdU/IdU and BrdU/CldU were detected with a mouse anti-BrdU (1:100; BD Biosciences, Franklin Lakes, NJ, USA) and a rat anti-BrdU (1:100; ABD Serotec, Kidlington, UK) antibody, respectively. Immunohistochemistry was performed as described (Garel et al., 1997). EdU incorporation was revealed using the Click-iT EdU Imaging Kit (Invitrogen).

Cell-cycle analysis

Cell-cycle progression in the cerebellum was analyzed as described (Takahashi et al., 1993). Cell-cycle phases in *Neurog2*$^{CreER/+}$ and *Neurog2*$^{CreER/CreER}$ were compared using a *t*-test for paired samples.

Histological procedures

Tissues were prepared as described (Croci et al., 2006). Mouse primary antibodies: calbindin, parvalbumin (1:1500; Swant, Bellinzona, Switzerland); SMI32 (1:250; Sternberger Monoclonals, Lutherville, MD, USA); NeuN (1:500; Millipore, Billerica, CA, USA); S100β (1:1000; Sigma); ER [1:100; Santa Cruz Biotechnology (SCB), Santa Cruz, CA, USA]; TuJ1 (1:300; Covance, Princeton, NJ, USA); MAP2 (1:300; BD Biosciences); and RC2 (1:20; DSHB, Iowa City, IO, USA). Rabbit primary antibodies: β-galactosidase (β-gal; 1:20,000; Cappel, Westchester, PA, USA); GFP (1:700; Invitrogen); calretinin (1:2500; Swant); neurogranin (1:250; Millipore); Olig2, PH3 (1:500; Millipore); ER (1:100; Thermo Fisher Scientific, Waltham, MA, USA); Dcx (1:100; SCB); NICD (1:100; Cell Signaling, Beverly, MA, USA); Pax2 (1:300; Invitrogen); GABA (1:2500; Sigma); and Vglut2 (1:100; Synaptic Systems, Goettingen, Germany). Chicken primary antibody: GFP (1:500; Abcam, Cambridge, UK). Goat primary antibody: Neurog2 (1:200; SCB).

For epitope unmasking, cryosections were boiled in 10 mM citrate buffer (pH 6) for 5 minutes. The Tyramide Signal Amplification Kit (Perkin Elmer, Waltham, MA, USA) was used to detect β-gal, Neurog2 and NICD.

Fate mapping analysis of *Neurog2*$^{+}$ progenitors

Neurog2$^{CreER/+}$ and *Rosa26*$^{lacZ/lacZ}$ mice were crossed. Pregnant females were injected i.p. with tamoxifen (TM; Sigma; 3-5 mg/25 g body weight). Progeny were harvested at E18, given to foster mothers and sacrificed at P30. Sections from mice receiving TM at E11.25 (TM$^{E11.25}$) (*N*=15,089 cells/3 cases), TM$^{E11.75}$ (*N*=5507 cells/2 cases) and TM$^{E12.25}$ (*N*=6919 cells/2 cases) were immunostained for β-gal and specific cerebellar markers, and *lacZ*-expressing cells from three series were quantitated.

Transplantation experiments

Donor cells were isolated and dissociated at E12.5 from *Neurog2*$^{CreER/+}$; *Rosa26*$^{lacZ/+}$ embryos (TM$^{E11.75}$) and grafted to wild-type P2 or P5 cerebella (Jankovski et al., 1996; Carletti et al., 2002). A single-cell suspension (1 μl at final concentration 5×10^4 cells/μl), obtained by mechanical dissociation of cerebellar primordia, was injected using a glass capillary. Grafted cells were recognized by β-gal expression. Phenotypes were scored as described (Carletti et al., 2002; Leto et al., 2006). Results from the same experimental set were pooled.

Wholemount *lacZ* staining

Wholemount *lacZ* staining was performed as previously described (Corradi et al., 2003).

Real-time quantitative PCR (RT-qPCR)

Total RNA was extracted from embryos at different stages using the RNeasy Micro Kit (Qiagen). Total RNA (1 μg) was retro-transcribed using first-strand cDNA M-MLV reverse transcriptase (Invitrogen) and random primers (Invitrogen) and 2 μl of 1:10 cDNA was used for each reaction. RT-qPCR was performed using the LightCycler 480 SYBR Green I Master Mix (Roche, Mannheim, Germany). Each gene was analyzed in triplicate. Data analysis was performed with the ΔΔCt method. All RNA levels were normalized to *Gapdh*. The following primers (5′-3′) were used: Gapdh-F, TGAAGCAGGCATCTGAGGG; Gapdh-R, CGAAGGTGGAAGAGTGGGAG; Neurog1-F, ATCACCACTCTCTGACCC; Neurog1-R, GAGGAAGAAAGTATTGATGTTGCCTTA; Ascl1-F, AGGAACAAGAGCTGCTGGAC; Ascl1-R, TCGTTGGCGAGAAACACTAA; Map2-F, AGCACTTGATTGGGAAGCACT; Map2-R, CGCCAATTCAAGGAAGTTGT; Sclip-F, AGACTGCAGCTCCCAGACAC; Sclip-R, AGCGACAGCACAGATAACTCC; Rora-F, CGAGCTCCAGCCGAGGTATCTCA; Rora-R, GCCCTTGCAGCCTTCACACGTAA.

Plasmid construction

The *flagNeurog2* cDNA (kind gift of M. Goetz, Helmholtz Center, Munich, Germany) was subcloned into pCCL.sin.cPPT.SV40polyA.eGFP.minCMV.hPGK.ΔLNGFR.WPRE (kind gift of L. Naldini, TIGET-San Raffaele, Milan Italy) replacing the ΔLNGFR sequence (Amendola et al., 2005).

Lentiviral (LV) vector production, titration and validation

VSV pseudotyped third-generation LVs were produced as described (Follenzi et al., 2000; Muzio et al., 2010). Expression titers, as determined on HEK293 cells by FACS analysis (FACSCalibur, BD Biosciences), were 3.6×10^9 TU/ml (control) and 2.4×10^9 TU/ml (flagNeurog2). Western blots of infected HEK293 lysates were hybridized for flagNeurog2 (flag M2, Sigma) and GFP (Molecular Probes, Eugene, OR, USA).

In utero LV delivery

Cntrl-GFP and *Neurog2-GFP* LVs were mixed with 0.01% Fast Green (Sigma) and injected in utero into the E12.5 fourth ventricle. Pregnant dams received a single CldU pulse before LV injection, and single EdU and IdU pulses 24 and 48 hours, respectively, thereafter. Brains were collected at E17.5.

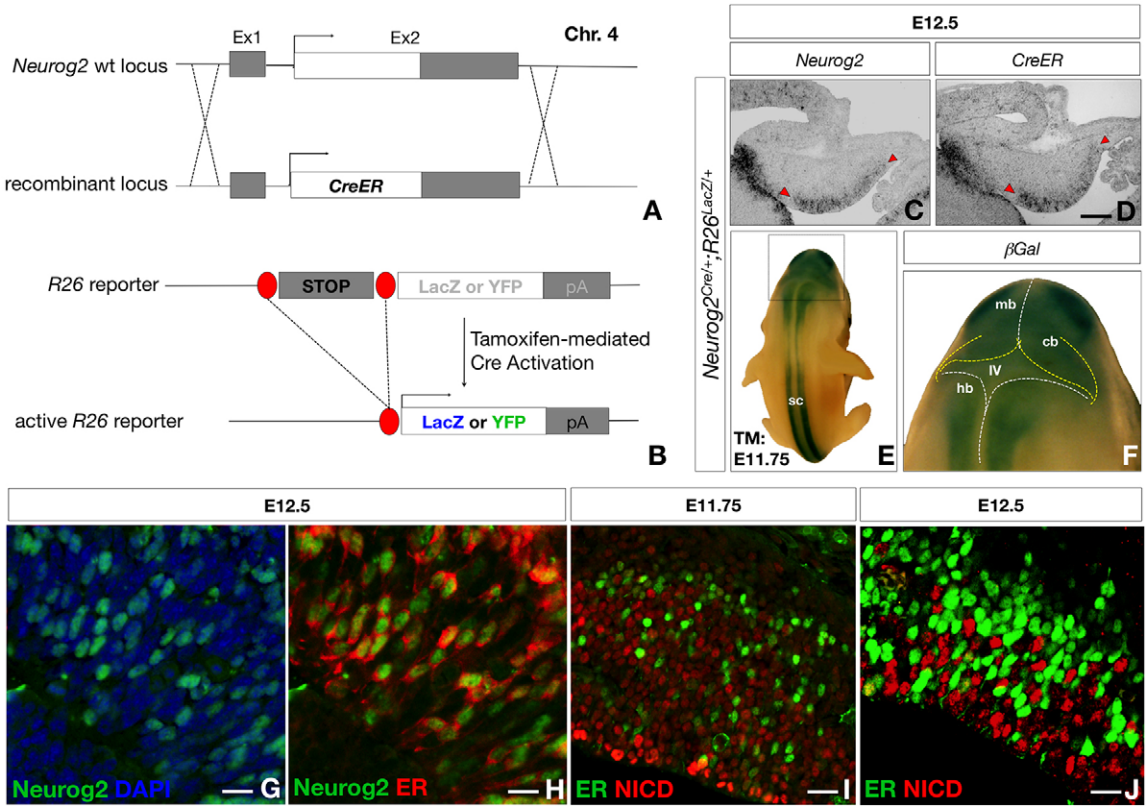

Fig. 1. Generation of the *Neurog2CreER* knock-in line. (**A**) The *Neurog2* wild-type (wt) coding sequence was replaced by a tamoxifen (TM)-inducible *CreER* gene. (**B**) Cre-dependent reporter activation. (A,B) Boxes indicate exons (white, coding; gray, untranslated); dotted lines, homologous recombination; ovals, loxP sites; Ex, exon; pA, poly(A). (**C**,**D**) In situ hybridization with *Neurog2* or *Cre* cRNAs in adjacent sagittal sections of *Neurog2*$^{CreER/+}$ embryonic cerebellum. Arrowheads indicate the anterior and posterior boundaries of *Neurog2* and *CreER* expression. (**E**,**F**) Wholemount X-Gal staining of a *Neurog2*$^{CreER/+}$; *Rosa26*$^{lacZ/lacZ}$ embryo (TM$^{E11.75}$). (**G-J**) *Neurog2*$^{CreER/+}$ cerebellar sagittal sections immunostained for Neurog2 and ER (G,H) or and NICD and ER (I,J). In H, ER labels cytoplasm (no TM). In I,J, ER labels nuclei (TM induced). Anterior is to the left. mb, midbrain; cb, cerebellum; hb, hindbrain; sc, spinal cord; IV, fourth ventricle. Scale bars: 90 μm in C,D; 10 μm in G,H; 20 μm in I; 15 μm in J.

PC dendrite development

For loss-of-function (LOF) experiments, E17.5 cerebellar sections from *Neurog2*$^{CreERT2/+}$; *Rosa26*$^{YFP/YFP}$ and *Neurog2*$^{CreERT2/CreERT2}$; *Rosa26*$^{YFP/YFP}$ embryos were analyzed. YFP$^+$ neurons were scored from random fields (5±1 neurons per field). In gain-of-function (GOF) experiments, E12.5 embryos were infected with vectors encoding either Neurog2 and GFP, or GFP alone. GFP$^+$ neurons were scored from random fields (5±2 neurons per field). In both GOF and LOF experiments, only neurons exhibiting detectable neurites were included in the analysis.

Sholl analysis was performed with ImageJ (NIH), using the Concentric Circles plug-in (rsbweb.nih.gov/ij/plugins/concentric-circles.html) and Sholl Analysis plug-ins (Ghosh laboratory, biology.ucsd.edu). Measurements were performed within seven concentric circles centered on the cell soma and spaced by 10 μm. Intersections within each concentric circle were counted, and average branch numbers were compared by means of a *t*-test. Results are presented as mean ± s.e.m.

Microarray analysis

E13.5 cerebellar primordia were dissected from wild-type and null embryos (n=3) to obtain total mRNA preparations (RNeasy Micro Kit, Qiagen). RNA (500 ng) was used for cRNA generation (Illumina Total Prep Kit, Ambion). Hybridization of MouseWG-6_V2 arrays (Illumina, Eindhoven, The Netherlands) was performed as recommended by the manufacturer. Image files were acquired on a BeadXpress scanner (Illumina). After data normalization and filtering, differentially expressed genes (significance threshold P<0.01; fold changes <0.7 or >1.7) were included in the analysis. Unsupervised hierarchical clustering showed that all transcriptional signatures correctly separated controls from nulls. The array contained 45,281 probes representing transcripts listed in the NCBI-Refseq, Riken and Meebo databases. Raw data were background-subtracted and cubic-spine-normalized using GenomeStudio GX software (Illumina) and further processed using MultiExperiment Viewer 4.7.1. (Saeed et al., 2006).

Statistical analysis

All experiments (including controls) were conducted in triplicate. Except where noted otherwise, statistical analysis was conducted using the unpaired Student's *t*-test and P<0.05 was used as the threshold for statistical significance.

RESULTS

Generation of *Neurog2*^{CreER} knock-in mice and genetic inducible fate mapping (GIFM)

The *Neurog2::ER*^{T2}*iCreER*^{T2} mouse line, which expresses tamoxifen (TM)-inducible Cre recombinase under the control of *Neurog2* cis-acting sequences (see Materials and methods; hereafter referred to as *Neurog2*^{CreER}), was produced by homologous recombination. As illustrated in Fig. 1A, exon 2, which is the only *Neurog2* coding exon, was replaced by the improved Cre recombinase (iCre) (Shimshek et al., 2002) fused in frame N- and C-terminally with the modified human estrogen

receptor (ER) termed T2 (Indra et al., 1999). This fusion protein (Casanova et al., 2002) displays high recombination efficiency in the presence of TM and very low background activity in its absence (Jullien et al., 2008).

Neurog2^{CreER} heterozygotes were bred into *Rosa26* Cre reporter lines, harboring either *lacZ* (Soriano, 1999) or *YFP* (Srinivas et al., 2001). Upon administration of TM, the Cre recombinase activates reporter gene expression (Fig. 1B). Reporter activity becomes detectable 12 hours after TM injection and increases thereafter, reaching a plateau between 18 and 24 hours (Fig. 1E,F and supplementary material Fig. S1A-C), in agreement with previous reports (Hayashi and McMahon, 2002).

Comparative analysis of *Neurog2* and *CreER* expression

The *Neurog2* transcript is detectable in the cerebellar primordium from E10.75 to E13.5, peaking between E11.5 and E12.5 (Zordan et al., 2008). We compared the distribution of *Neurog2* and *CreER* transcripts in the cerebellar primordium of *Neurog2$^{CreER/+}$* embryos by in situ hybridization and showed that the *CreER* and *Neurog2* territories overlap (Fig. 1C,D). To demonstrate colocalization of Neurog2 and CreER proteins, we immunostained E12.5 *Neurog2$^{CreER/+}$* cerebellar sections. Our results indicate that Neurog2 and ER colocalize in an overwhelming majority of cells (Fig. 1H). Thus, in this study, ER staining will be considered synonymous with Neurog2 distribution.

Neurog2 is expressed by dividing progenitors in the cbVZ

In the embryonic telencephalon, *Neurog2* is expressed in a salt-and-pepper pattern due to Notch-mediated lateral inhibition. The expression of Neurog2 and of Notch effectors (such as Hes genes) in neural progenitors are inversely correlated (Shimojo et al., 2008). However, no information is available as regards the embryonic cerebellum. We compared the distributions of ER and Notch intracellular domain (NICD) in the cbVZ of E11.5 and E12.5 *Neurog2$^{CreER/+}$* embryos. Our results indicate that, at both stages, ER expression is virtually restricted to NICD-negative progenitors (Fig. 1I,J).

Basic helix-loop-helix (bHLH) proteins are known to function as master regulators of mammalian neurogenesis, linking neuronal differentiation to cell-cycle regulation (Farah et al., 2000). To determine whether *Neurog2* in the cbVZ is expressed by cycling progenitors or by postmitotic neurons, we immunostained for ER and the early postmitotic marker Tuj1 (Tubb3 – Mouse Genome Informatics) (supplementary material Fig. S2A-D). Only a small minority of *Neurog2^{+}* cells stained positive for TuJ1 [8.6±4.2% (mean ± s.d.); plotted in supplementary material Fig. S2E], indicating that *Neurog2* is almost exclusively expressed by dividing cells.

Characterization of cell-cycle parameters in the E12.5 cbVZ

As they progress through the cell cycle, apical progenitor nuclei undergo interkinetic migration along the apical-basal axis, with mitoses occurring at the apical surface and S phase taking place at a basal location, with apical-to-basal nuclear migration in G1 phase and the reverse in G2 phase (Sauer and Walker, 1959). Restricted *Neurog2* distribution in the cbVZ (Zordan et al., 2008) suggests that, in cerebellar neurogenesis, *Neurog2* transcription might be cell cycle dependent, and that lack of *Neurog2* might hamper cell-cycle progression. However, no information is available to date as regards cell-cycle kinetics in the cbVZ. We analyzed cell-cycle parameters in cbVZ progenitors, then applied our results to the evaluation of cell-cycle kinetics in *Neurog2* nulls.

Cumulative S-phase labeling was achieved by pulsing E12.5 embryos every 3 hours with EdU. The labeling index (ratio of labeled nuclei to total nuclei, LI) was plotted at each time point. The growth fraction (ratio of proliferating to total cells, GF), overall cell-cycle length (T_C) and S-phase length (T_S) were calculated as described (Nowakowski et al., 1989). T_C–T_S corresponds to the interpolated value at which LI reaches GF. GF, T_C and T_S were calculated based on the value of the *y* intercept [$(T_S/T_C)\times GF$] and on the time at which the asymptote was reached (T_C–T_S, i.e. the time required to label the complete GF) (Takahashi et al., 1995). At E12.5, T_C equaled 13.9 hours, with an 85% GF and 9 hours to reach GF (T_C–T_S). T_{G2+M} length was estimated as 2 hours (Takahashi et al., 1993); the length of G1 was calculated by subtracting T_S+T_{G2+M} from T_C. The resulting cell-cycle durations were: T_{G1}, 7.0 hours; T_S, 4.9 hours; T_{G2+M}, 2 hours (Table 1).

These results were used to map the cell-cycle stage(s) at which *Neurog2* is expressed in E12.5 *Neurog2$^{CreER/+}$* embryos (Britz et al., 2006; Shimojo et al., 2008; Sunabori et al., 2008). Sections were immunostained for ER and EdU. *Neurog2^{+}* S-phase progenitors (ER^{+} EdU^{+}/total ER^{+}) were labeled through a single 30-minute pulse (EdU$^{30'}$) prior to sacrifice; 4.9±3.1% of *Neurog2^{+}* progenitors were EdU positive (Fig. 2A,A′). For S+G2+M phase, embryos were labeled by EdU^{3hours}; 8.4±6% of ER^{+} progenitors were EdU^{+} (Fig. 2B,B′), with hardly any double-positive cells located at the apical surface (M phase). Accordingly, only 0.8±0.5% stained double positive for ER and phospho-histone H3 (PH3) (Fig. 2C,C′). Progenitors located in early and late G1 were labeled by EdU^{8hours} and EdU^{14hours}; 24.4±9.8% of ER^{+} progenitors stained positive for EdU using EdU^{8hours} (Fig. 2D,D′), whereas 63.4±10.6% of ER^{+} progenitors colocalized with EdU using EdU^{14hours} (Fig. 2E,E′), indicating a specific enrichment of *Neurog2* expression in late G1-phase progenitors. Although similar studies have been conducted in other brain regions (Miyata et al., 2004; Britz et al., 2006; Yi et al., 2008), this is an entirely novel finding in the context of cerebellar neurogenesis.

The restriction point (RP) is a cell-cycle checkpoint that occurs after early G1. Cells passing through RP re-enter S phase, while the others enter G0 (the G1/G0 transition) and start differentiating (Takahashi et al., 1999). To determine whether *Neurog2^{+}* progenitors in late G1 are poised to leave the cell cycle, E11.75 *Neurog2$^{CreER/+}$; Rosa26$^{YFP/+}$* embryos were TM treated and cerebella collected at E12.5, after an EdU$^{30'}$ pulse. All Neurog2^{+} YFP^{+} progenitors examined stained positive for the postmitotic markers TuJ1 and Dcx (supplementary material Fig. S3A,B). Hardly any cells (<0.2%) were double positive for YFP and dividing radial glia markers, such as RC2 (Ifaprc2 – Mouse Genome Informatics) (supplementary material Fig. S3C), Blbp (Fabp7 – Mouse Genome Informatics) or nestin (not shown), and virtually no tagged progenitors (<0.1%)

Table 1. Cell-cycle parameters of E12.5 *Neurog2$^{CreER/+}$* versus *Neurog2$^{CreER/CreER}$* cbVZ progenitors

	Cell-cycle parameters (hours)					
Genotype	T_C–T_S	T_S	T_C	T_{G2+M}	T_{G1}	GF (%)
Neurog2$^{Cre/+}$	9	4.9	13.9	<2.0	>7.0	85±5
Neurog2$^{Cre/Cre}$	11	5.8	16.8	<2.0	>9.0	84±3

Cell-cycle parameters were calculated according to Nowakowski et al. (Nowakowski et al., 1989).
GF, growth fraction (shown as mean±s.d.); T_C, total length of the cell cycle; T_S, length of S phase; T_{G2+M}, length of G2 plus M phase; T_{G1}, length of G_1 phase.

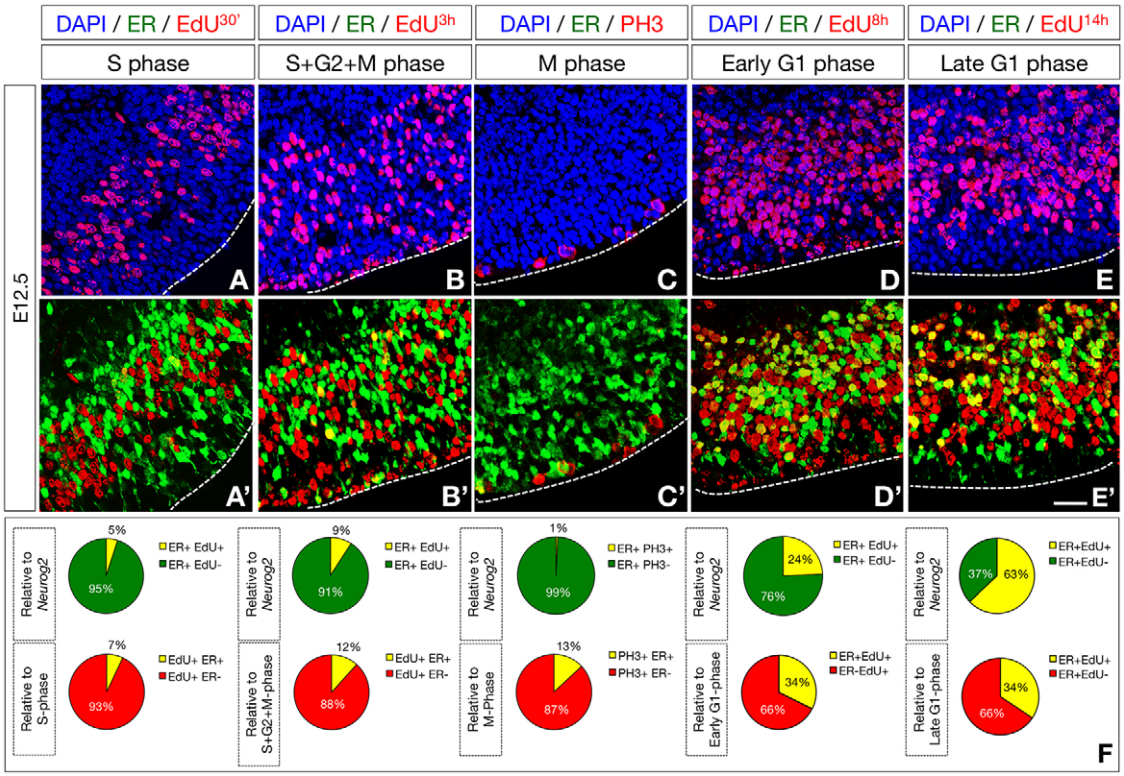

Fig. 2. *Neurog2* expression is restricted to progenitors undertaking G1/G0 phase transition. (**A-E′**) Sagittal sections of the *Neurog2*$^{CreER/+}$ cbVZ immunostained for ER and EdU, pulsed at different time points before harvesting. (A,A′) EdU$^{30'}$ labels ER$^+$ S-phase nuclei. (B,B′) EdU^{3hours} labels ER-positive S, G2 and M nuclei. (D,D′) EdU^{8hours} labels ER$^+$ early G1 nuclei. (E,E′) EdU^{14hours} labels ER$^+$ late G1 nuclei. (C,C′) ER$^+$ M-phase nuclei, counterstained for PH3. Anterior is to the left. The dashed line delineates the apical margin of the cbVZ. (**F**) Percentages of ER$^+$ EdU$^+$ progenitors at each cell-cycle phase, expressed as a fraction of either total ER$^+$ (top, ER$^+$ EdU$^+$/total ER$^+$) or total EdU$^+$ (bottom, ER$^+$ EdU$^+$/total EdU$^+$) cells. Scale bar: 30 μm.

colocalized with either PH3 or EdU (supplementary material Fig. S3D-F). In the *Neurog2*$^{CreER/+}$*; Rosa26*$^{lacZ/+}$ line, reporter activity is detectable 12 hours after TM administration (supplementary material Fig. S1A). In the E12.5 cbVZ, the cell cycle lasts ~14 hours. If any cells were to re-enter S phase due to high CreER protein levels, then reporter activity would be detected in the cbVZ. Our results indicate that progenitors that become robustly positive for *Neurog2* leave the cell cycle almost immediately and undertake differentiation and radial migration. In other words, in the cbVZ, *Neurog2* is overwhelmingly expressed by G1 progenitors that are bound to withdraw from the cycle.

Neurog2 null progenitors stall in early G1, resulting in a slower cell cycle

Cumulative S-phase labeling revealed a significant decrease in the rate of cell-cycle progression in the *Neurog2* null cbVZ. At E12.5, T_C was increased by 2.9 hours (Fig. 3A,G), and T_{G1} and T_S by 2 and 0.9 hours, respectively (P=0.02, Table 1). CreER distribution was unaffected in S, G2 and M, with only sparse ER$^+$ progenitors detected at these stages (plotted in Fig. 3F). However, striking differences became apparent in G1. Specifically, *Neurog2*$^{CreER/CreER}$ exhibited an increase in ER$^+$ progenitors in early G1 versus controls (EdU^{8hours}, 60.4±9.1% versus 24.4±9.8%; P<0.01; Fig. 3B′,C′,F), with a corresponding decrease in the late G1 fraction (EdU^{14hours}, 31.3±15.5% versus 63.4±9.8%; P<0.01; Fig. 3D′,E′,F). Accordingly, ER$^+$ *Neurog2* null nuclei were detected in a more apical position relative to their wild-type counterparts (supplementary material Fig. S4), suggesting that *Neurog2* null progenitors stall in their progression through G1. An alternative scenario is that *Neurog2* knockout elicits a feedback upregulation of the *Neurog2* promoter in early G1 progenitors. At odds with this possibility, the total number of ER$^+$ progenitors is not significantly increased in *Neurog2* null cerebella. Thus, *Neurog2* appears to affect cell-cycle kinetics by modifying the pace of early to late G1 transition (Fig. 3G). As in controls, YFP$^+$ *Neurog2* null E12.5 progenitors (TM$^{E11.75}$) do not re-enter the cell cycle and instead become postmitotic, indicating that the delay in G1 progression does not ultimately prevent cell-cycle exit (not shown).

Next we asked whether other proneural genes undergo a compensatory upregulation in the *Neurog2* null cbVZ. RT-qPCR revealed a significant upregulation of both *Ascl1* and *Neurog1* (Fig. 3H). These results are in keeping with recent findings showing that *Ascl1* rescues the stall of neurogenesis observed in the developing retina of *Neurog2* null mutants (Hufnagel et al., 2010).

Neurog2 overexpression accelerates cell-cycle withdrawal

To confirm the evidence obtained in *Neurog2* nulls, we took a GOF approach. The fourth ventricle of E12.5 wild-type embryos was injected with a lentivirus (Amendola et al., 2005) encoding *Neurog2* and *GFP* (hereafter referred to as *Neurog2-GFP* LV) or with a control *GFP* vector. Embryos were pulsed with CldU, EdU and IdU (1 hour before, 24 and 48 hours after injection,

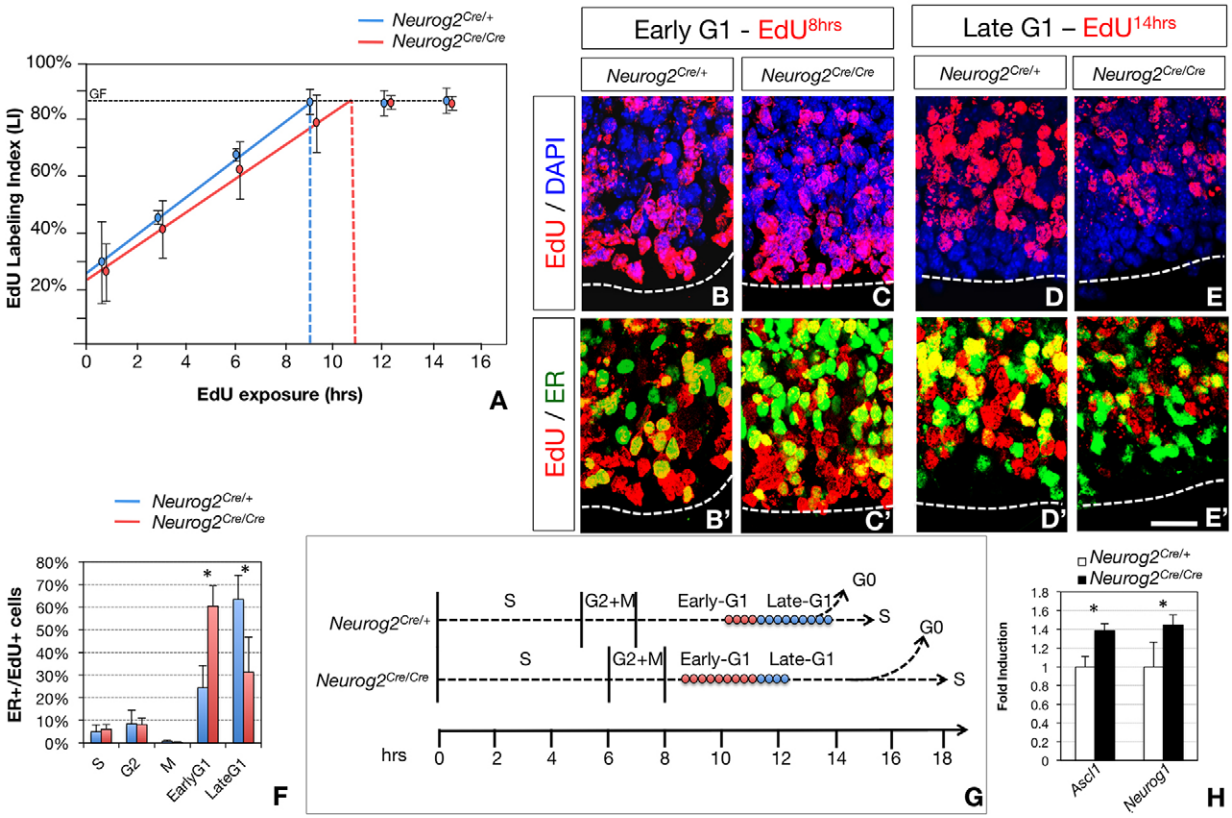

Fig. 3. *Neurog2* null progenitors stall in the transition between early and late G1. (**A**) Cumulative labeling of cbVZ progenitors. Blue, *Neurog2*$^{CreER/+}$; red, *Neurog2*$^{CreER/CreER}$. In *Neurog2*$^{CreER/CreER}$ cbVZ, the labeling index (LI) reaches the growth fraction (GF) value later than in controls (coefficients of determination R^2 are 0.948 and 0.977, respectively; $P<0.02$, dependent *t*-test for paired samples). (**B-E′**) Matched sagittal sections of *Neurog2*$^{CreER/+}$ versus *Neurog2*$^{CreER/CreER}$ cbVZ immunostained for ER and EdU. (B-C′) EdU^{8hours} labels early G1-phase nuclei. (D-E′) EdU^{14hours} labels late G1 phase. A corresponding increase in the fraction of *Neurog2* null ER$^+$ progenitors (C,C′) is detected in early G1, compared with controls (B,B′). (**F**) Percentages of ER$^+$/EdU$^+$ colocalization in each cell-cycle phase. The fraction of ER$^+$ progenitors in late G1 is significantly decreased in the *Neurog2* null cbVZ (red) versus the control cbVZ (blue) (*$P<0.005$, independent two-sample *t*-test). (**G**) Schematic representation of cell-cycle progression in *Neurog2* nulls versus controls. Dots represent G1 progenitors. A higher percentage (60.4%) of null progenitors stall in early G1 (red dots) during their progression to late G1/G0 (blue dots). (**H**) RT-qPCR shows significant upregulation of *Ascl1* and *Neurog1* in *Neurog2* null cerebellar primordium at E12.5 (1.4- and 1.43-fold, respectively; *$P<0.05$). Mean ± s.e.m. Scale bar: 20 μm.

respectively) and E17.5 cerebella were immunostained for GFP and EdU. The LI profile of *Neurog2-GFP* LV-infected cells is represented for each time point in Fig. 4D, revealing that the GFP$^+$ EdU$^+$ population was strikingly reduced in *Neurog2-GFP* LV-infected cells as compared with controls (Fig. 4A,B). Thus, *Neurog2* overexpression accelerates cell-cycle withdrawal, exhausting the proliferating pool.

Fate mapping of *Neurog2*$^+$ progenitors

Although *Neurog2* is expressed in a portion of the *Ptf1a* expression domain, the contribution given by *Neurog2*$^+$ progenitors to the mature cerebellum is unknown. We used the *Neurog2*$^{CreER/+}$; *Rosa26*$^{lacZ/+}$ line to tag *Neurog2*$^+$ progenitors and follow their eventual fate in the adult cerebellum. Embryos were TM treated at three different stages spanning the *Neurog2* expression window (TM$^{E11.25}$, TM$^{E11.75}$, TM$^{E12.25}$). β-gal-tagged cells were visualized on P30 and identified via cerebellar neuron markers (Fig. 5A-P).

At all induction stages, *Neurog2*$^+$ precursors yielded three GABAergic neuron classes: (1) a vast majority of PCs (Fig. 5A-I); (2) SMI32$^+$ (SMI32 detects non-phosphorylated neurofilament H) presumptive nucleo-olivary neurons (Leto et al., 2006) (Fig. 5L,M); and (3) calretinin$^+$ (calbindin 2 – Mouse Genome Informatics) dorsal cochlear nucleus (DCN) interneurons (Fig. 5N). At E12.5, a small subset of Neurog2$^+$ β-gal$^+$ progenitors (TM$^{E11.75}$) also expresses Pax2 (Fig. 5Q,S), a marker of all cerebellar GABAergic interneuron precursors (Maricich and Herrup, 1999; Leto et al., 2006; Carletti et al., 2008). Cortical GABAergic interneuron types (Golgi, Lugaro, basket and stellate) were virtually absent from the tagged neuronal pool (<1%). Finally, *Neurog2*$^+$ progenitors gave rise to a small percentage of S100β$^+$ Bergmann glial cells (Fig. 5O), possibly as products of symmetric, self-consuming radial glial division. Distributions of cerebellar cell types for each stage are plotted in Fig. 5P.

Transplanted *Neurog2*$^+$ progenitors are cell-autonomously committed to PC and DCN neuron fates

Fate mapping suggests that *Neurog2*$^+$ progenitors are lineage restricted, producing only a defined subset of cerebellar neurons, primarily PCs. When heterochronically transplanted to the postnatal cerebellum, E12.5 cbVZ progenitors generate the entire repertoire of cerebellar neurons (Carletti et al., 2002; Carletti and Rossi, 2008; Williams et al., 2008). To determine whether E12.5 *Neurog2*/β-gal-tagged progenitors (TM$^{E11.75}$) are cell-

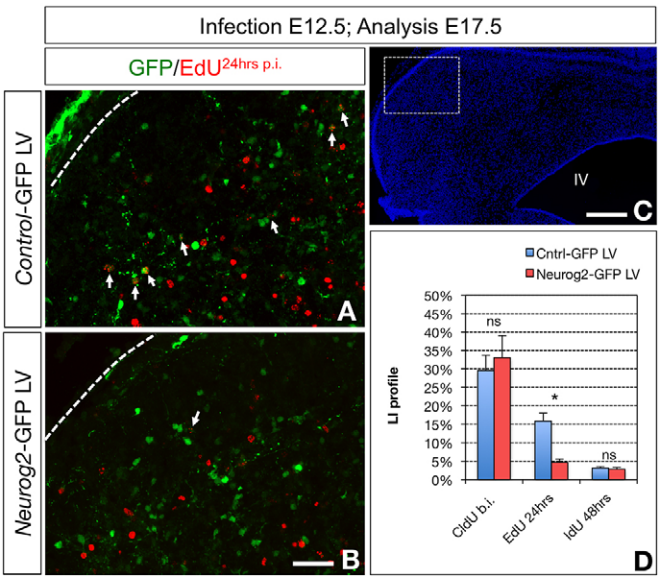

Fig. 4. *Neurog2* overexpression promotes cell-cycle withdrawal in the cbVZ. (**A**,**B**) Coronal matched sections of E17.5 cerebella infected at E12.5 with either *Cntrl-GFP* LV (A) or with *Neurog2-GFP* LV (B). Embryos were single-pulsed with CldU 1 hour before injection (b.i.), and with EdU and IdU 24 and 48 hours post infection (p.i.), respectively. Sections were immunostained for GFP and either CldU, EdU (A,B) or IdU. Arrows indicate GFP$^+$ cells positive for EdU. (**C**) DAPI staining of a coronal hemicerebellar section. IV, fourth ventricle. Inset indicates approximate location of A and B. (**D**) The LI profile of *Neurog2-GFP* LV-infected cells shows that the fraction of GFP$^+$ EdU$^+$ cells is reduced by 71.8% as compared with controls, indicating a marked depletion of the dividing progenitor pool (*P<0.01, independent two-sample t-test). ns, not significant. Mean ± s.e.m. Scale bars: 30 μm in A,B; 100 μm in C.

autonomously restricted to their endogenous fates or acquire late-generated interneuron identities, we grafted them to wild-type cerebella at P2 and P5 and examined the resulting phenotypic repertoires at P30. Embryonic donor cells either reaggregated into mini-cerebellar structures (Fig. 6A-D) or engrafted as isolated scattered elements (Fig. 6E-O) (Jankovski et al., 1996). At both stages, grafted (Fig. 6P,Q) donor β-gal$^+$ cells differentiated exclusively into PCs (83.4±7.6%; Fig. 6A-J) or DCN GABAergic neurons (14.0±3.9%; Fig. 6N,O). β-gal$^+$ cells did not incorporate BrdU pulsed immediately after transplantation (Fig. 6K-M), confirming that they are postmitotic. This indicates that *Neurog2*$^+$ progenitors are, to a large extent, cell-autonomously committed to adopt PC and DCN neuron fates.

Neurog2 acts redundantly in PC fate specification

To determine whether *Neurog2* is required for cbVZ progenitors to adopt a PC fate, we compared the identity of β-gal-tagged neurons in *Neurog2*$^{CreER/+}$; *Rosa26*$^{lacZ/+}$ versus *Neurog2*$^{CreER/CreER}$; *Rosa26*$^{lacZ/+}$ embryos (TM$^{E11.75}$) at E17.5, using FoxP2 for PCs and DCN neurons, Pax2 for all types of GABAergic interneurons, Pax6 for GC precursors and S100β for astroglia. No relevant trans-specification was observed in null mutant cerebella: *Neurog2* null neurons correctly differentiated into FoxP2$^+$ PCs. Likewise, LV overexpression of *Neurog2* did not affect the number of PCs in the E17.5 cerebellum (data not shown). Thus, *Neurog2* may either play a minor role in PC fate specification or act redundantly with other proneural genes.

The total number of PCs is reduced in postnatal *Neurog2* null mutants

Although pure-bred *Neurog2* nulls die around birth (Fode et al., 1998; Fode et al., 2000; Hand et al., 2005), some outbred mutants survive until P15 (Andersson et al., 2006). In surviving mutants, null cerebella are decreased in volume (by 20%; Fig. 7) and exhibit a lobulation defect (Fig. 7A,C-C″) both in the vermis (lobules VI, VII and IX) and hemispheres (fusion of crus 1 and simplex lobule). The thickness of all cortical layers is also reduced (Fig. 7D; see Discussion) and PC number is decreased by 20%, whereas PC density is unaffected (Fig. 7E). TUNEL staining conducted at E14.5 and E17.5 was unchanged (data not shown). As regards PC subtypes, *Neurog2* expression does not match the distribution of zebrin II (Aldoc – Mouse Genome Informatics), which is the main marker of parasagittal domains in the cerebellum (supplementary material Fig. S5). Further studies are required to determine whether *Neurog2* deletion affects any specific PC subpopulations.

Neurog2 regulates PC dendritogenesis

Next, we assessed whether *Neurog2* regulates PC differentiation. Embryos (TM$^{E11.75}$) were analyzed at E17.5, at the end of PC migration. At this stage, PCs adopt a bipolar elongated shape, develop a branched apical dendrite and start generating new and thinner processes radiating from the cell body (Sotelo and Rossi, 2011). *Neurog2* null PCs migrate normally underneath the external granular layer. However, they exhibit a striking reduction in neurite branching. Compared with control PCs, which are fusiform in shape and have extensively branched processes, *Neurog2* null PCs are round, with simple and stunted neurites, if any, as shown by YFP and MAP2 (Mtap2 – Mouse Genome Informatics) co-immunostaining (Fig. 8A-B′).

As illustrated in Fig. 8C and plotted in Fig. 8D, less than 1% of mutant PCs exhibited a branched apical dendrite, while 47% carried a single stunted process stemming from the cell soma, and 52% lacked any surface processes. Conversely, all control PCs had an elongated dendrite featuring 1, 2 or 3 or more main branches (20, 54 or 25%, respectively). Accordingly, *Neurog2*-overexpressing PCs exhibited a dramatic increase in process branching as compared with controls (Fig. 8H-J). Changes in dendritic branching were quantitated by Sholl analysis (Ristanovic et al., 2006), revealing a significant reduction in both the total length and average number of dendrites in *Neurog2* null PCs (Fig. 8G), whereas *Neurog2*-overexpressing PCs exhibited a sharp increase in both the length and number of dendritic processes (Fig. 8K). In the cerebellar primordium, *Neurog2* expression is detectable by RT-qPCR until E15 (Ct=32.5±0.07).

The expression of several established genetic regulators of early PC dendritic growth was examined in wild-type and null embryos by RT-qPCR of E14.5 cerebellar RNAs. Three genes were found to be downregulated in the *Neurog2* null cerebellum: *Rora* and *Sclip* (*Stmn3* – Mouse Genome Informatics), which are known to control the early stages of PC dendritogenesis (Boukhtouche et al., 2006; Poulain and Sobel, 2007), and *Map2*, which encodes a cytoskeletal protein involved in dendritic outgrowth and stabilization (Fig. 8L). All three genes are expressed in early postmitotic neurons, suggesting that *Neurog2* might act upstream of them as a master regulator of the intrinsic phase of PC dendritogenesis. While the above genes were downregulated in *Neurog2* null embryos at E14.5, the expression of many others was found to vary in a microarray analysis of wild-type versus null cerebella at E13.5, a stage spanning the end of PC neurogenesis

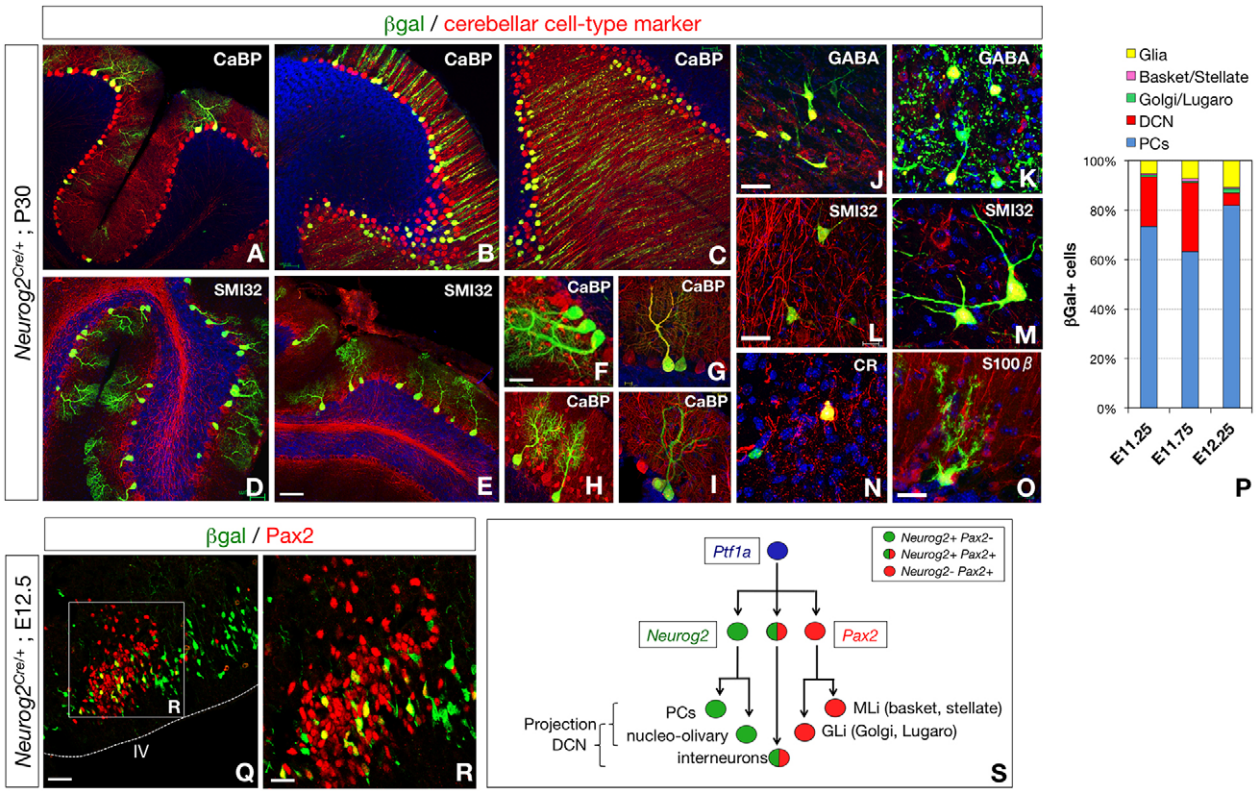

Fig. 5. Contribution of *Neurog2*$^+$ progenitors to the assembly of the mature cerebellar cytoarchitecture. (**A-O**) Analysis of Neurog2$^+$ β-gal$^+$ progenitors in *Neurog2*$^{CreER/+}$; *Rosa26*$^{lacZ/lacZ}$ P30 cerebella. (A-C) TM was administered at E11.25 (TM$^{E11.25}$); (J-M,Q) TM$^{E11.75}$; (D-I,N,O) TM$^{E12.25}$. (A-I) The majority of *Neurog2*$^+$ progenitors are fated to give rise to calbindin (CaBP)$^+$ (A-C,F-I), SMI32$^+$ (D,E) PCs. (J,K) Virtually all tagged cell bodies in DCN are GABA positive. (L,M) β-gal$^+$ DCN neurons that are SMI32$^+$. (N) Calretinin (CR) marks GABAergic DCN interneurons. (O) A very infrequent s100β$^+$ Bergmann glial cell. (**P**) Distribution of cerebellar cell types expressed as a fraction of total β-gal$^+$ cells for each stage of TM-induction. (**Q**,**R**) Sagittal section of E12.5 cbVZ from a *Neurog2*$^{CreER/+}$; *Rosa26*$^{lacZ/+}$ embryo (TM$^{E11.75}$). A small subset of β-gal-tagged progenitors stains positive for Pax2. (**S**) Lineage relationships linking *Neurog2*$^+$ cbVZ progenitors and GABAergic neuron subtypes in the mature cerebellum. This diagram does not reflect the temporal sequence of cell birth. Scale bars: 50 μm in A-E; 25 μm in F; 40 μm in G-J; 30 μm in K,L,Q; 20 μm in M-O; 15 μm in R.

and the onset of PC differentiation (supplementary material Fig. S6). An in-depth analysis of these results is in progress and is beyond the scope of the present paper.

At the end of development, PCs feature monoplanar, highly branched dendrites and are characterized by their apical dendritic tree, which stems from a single vertically oriented primary dendrite (Fig. 9A,C). We analyzed the long-term effects of *Neurog2* knockout on PC dendritogenesis in outbred *Neurog2* mutants. At P10, the dendrites of null mutant PCs, as stained with SMI32 antibody, are still dramatically stunted. Many *Neurog2* null PCs have thinned primary dendrites and a poorly branched arbor (Fig. 9B,D). Climbing fiber terminals, as stained with Vglut2 (Slc17a6 – Mouse Genome Informatics) antibody, impinge upon the main dendrites of both wild-type and mutant neurons (Fig. 9E,F), indicating that the defective dendritic development does not abolish PC innervation.

DISCUSSION

Here, we describe a new knock-in line and its analysis aimed at characterizing the roles of *Neurog2* in cerebellar development. This model, which permits the long-term stage-specific tagging of *Neurog2*$^+$ progenitors and of their adult derivatives, will facilitate developmental and transplantation studies, making it possible to assess the ability of Neurog2-tagged progenitors to integrate into the postnatal and adult CNS.

For the first time, we show that *Neurog2* is expressed by dividing NICD-negative progenitors in the cbVZ. Thymidine analog incorporation indicates that the early to late G1 transition is slower in *Neurog2* nulls and, accordingly, that *Neurog2* overexpression accelerates cell-cycle withdrawal, depleting the progenitor pool. Thus, *Neurog2* acts astride the G1 restriction checkpoint to affect cell-cycle progression in the cbVZ.

GIFM shows that all progenitors robustly expressing *Neurog2* exit the cell cycle and upregulate early differentiation markers within 12-24 hours. Thus, although *Neurog2* expression may oscillate repeatedly at low levels in the cbVZ [as shown in telencephalic neurogenesis (Shimojo et al., 2008)], when it reaches robust expression levels it dictates cell-cycle withdrawal. Interestingly, although *Neurog2* is expressed exclusively in daughter cells fated to exit the cell cycle, cellular progeny bound for cell-cycle re-entry are also delayed, suggesting non-cell-autonomous regulation.

Although *Neurog2* null progenitors are delayed in cell-cycle progression, with a decrease in neuronal output, *Neurog2* knockout does not completely abolish PC generation, possibly owing to compensatory *Neurog1* and *Ascl1* upregulation. As a result of the decreased PC progenitor output, the entire cerebellar cortex is thinner in null mutants. This is not surprising because, starting shortly before birth, PCs promote clonal expansion of GC progenitors (e.g. Wechsler-Reya and Scott, 1999). Thus, a

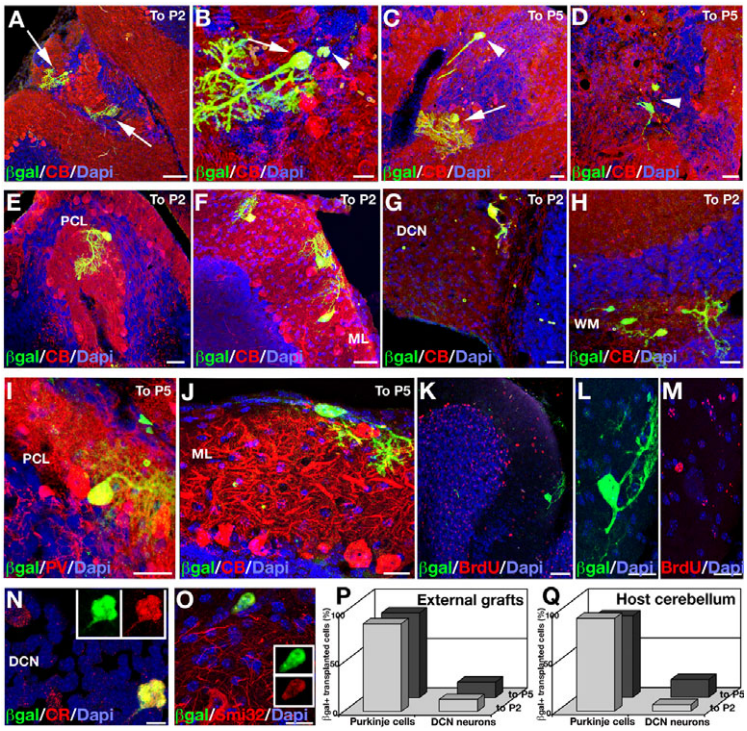

Fig. 6. Fate potential of *Neurog2*$^+$ progenitors after heterochronic transplantation. E12 *Neurog2*$^+$ cerebellar progenitors (TM$^{E11.75}$) were transplanted into postnatal recipient cerebella. (**A-D**) Some donor cells aggregate into mini-cerebellar structures adjacent to the external surface. Tagged cells were PCs (arrows in A-C) and neurons compatible with an immature PC identity (arrowheads in B-D). (**E-J**) Donor-derived PCs (not aggregated) integrated into the recipient PC layer (E,I) or homed ectopically in the host molecular layer (F,J), deep cerebellar nuclei (G) and white matter (H). (**K-M**) No grafted cell showed immunoreactivity for BrdU, as administered to the host immediately after transplantation. (**N**,**O**) Grafted *Neurog2*$^+$ progenitors also yielded CR$^+$ DCN interneurons (red in N) and SMI32$^+$ neurons (red in O), as highlighted in insets. (**P**,**Q**) Distribution of tagged cells located in external grafts (P) or integrated into the host cerebellum (Q). ML, molecular layer; PCL, Purkinje cell layer; WM, white matter; DCN, deep cerebellar nuclei. Scale bars: 100 μm in A; 20 μm in B,J,O; 30 μm in C,D,H,I; 40 μm in E; 50 μm in F,G,K; 25 μm in L,M; 10 μm in N.

reduction in PC numbers or a decrease in mitogen secretion by PCs is expected to translate into fewer GCs and a thinner molecular layer occupied by GC axons. Taken together, our findings establish that *Neurog2* plays an important role in PC development by regulating cell-cycle progression and neuronal output, a novel finding in cerebellar development.

Long-term GIFM indicates that *Neurog2*$^+$ progenitors give rise mainly to PCs and also to GABAergic DCN projection neurons, i.e. to the entirety of cerebellar GABAergic projection neurons. Moreover, the combination of Neurog2 and Pax2 expression at E12.5 represents the earliest known genetic signature of cerebellar DCN interneurons, an important foundation for future studies of cerebellar neurogenesis. Likewise, grafting experiments indicate that E12.5 *Neurog2*$^+$ progenitors are committed to a restricted set of neuronal identities. When grafted to the postnatal cerebellum, E12.5 *Neurog2*$^+$ precursors are cell-autonomously fated to PC or DCN neuron identities and they fail to acquire other interneuron fates. This indicates that *Neurog2*$^+$ cbVZ precursors are irreversibly committed to a positional identity code and mature by unfolding a cell-intrinsic ontogenetic program.

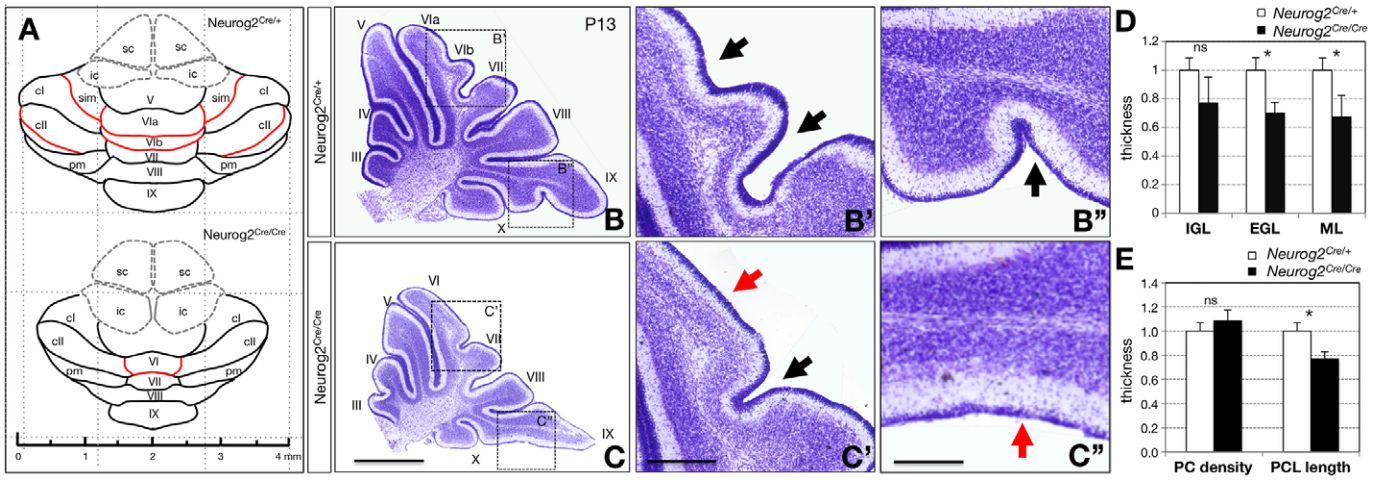

Fig. 7. Size reduction and lobulation defects in the *Neurog2* null cerebellum. (**A**) Summary of lobulation defects of P13 *Neurog2* null cerebella (bottom) versus wild-type controls. In the mutant hemispheres, the simplex lobule is not recognizable, while in the vermis the anterior lobe and lobules VI and VII are hypoplastic. (**B-C″**) Sagittal sections of wild-type (B-B″) and *Neurog2* null (C-C″) lateral vermis. Arrows point to defects in lobules VI and VII (C′ versus B′) and IX (C″ versus B″). (**D**) The external granular layer (EGL) and molecular layer (ML) are significantly thinner in the null cerebellum (*P<0.02). (**E**) The length of the PC layer is significantly reduced in the *Neurog2* null (*P<0.05), whereas PC density is unaffected. IGL, internal granular layer. Mean ± s.e.m. cl, crus I; cll, crus II; pm, paramedian; sim, simplex; ic, inferior colliculus; sc, superior colliculus. Scale bars: 1 mm in B,C; 200 μm in B′,C′; 100 μm in B″,C″.

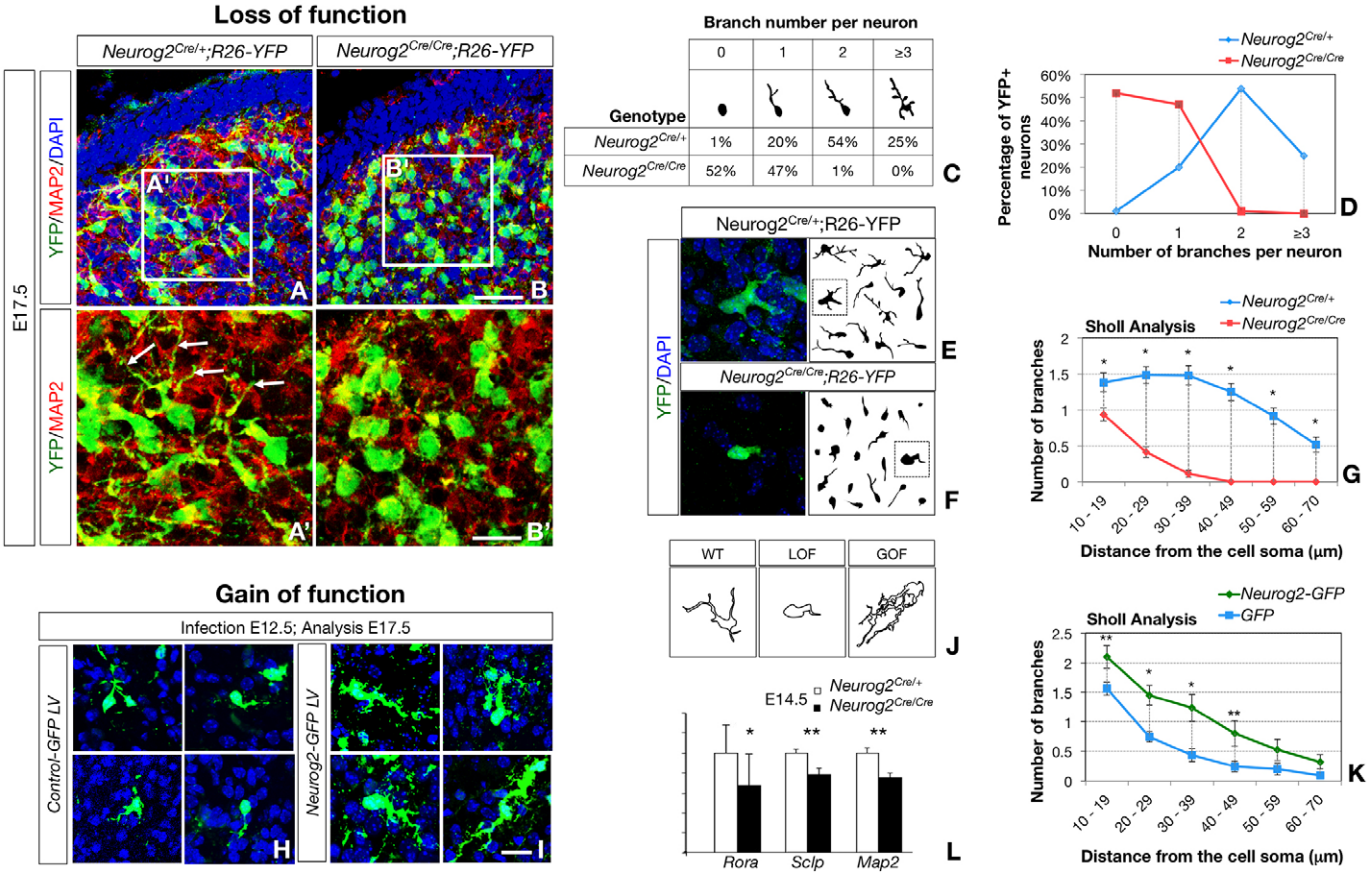

Fig. 8. *Neurog2* regulates PC dendritogenesis. (**A-G**) *Neurog2* loss-of-function. Compared with controls (A,A′,E), mutant PC dendrites are significantly shorter and less branched (B,B′,F). A majority of mutant neurons are round in shape with only a short process stemming from the cell soma (illustrated in C, quantitation in D; $P<0.001$). (G) Sholl analysis of PC dendrites from *Neurog2* null and wild-type PCs. $*P<0.01$. (**H-K**) *Neurog2* gain-of-function. (H,I) *Neurog2*-overexpressing PCs (I) exhibited an increase in process branching compared with controls (H). Representative profiles are illustrated in J. (K) Sholl analysis of *Neurog2*-overexpressing neurons versus controls. $*P<0.003$; $**P<0.02$. (**L**) RT-qPCR of *Rora*, *Sclip* (*Sclp*) and *Map2* transcript levels in wild-type versus *Neurog2* null mutant cerebella. $*P<0.01$ (5 embryos, in triplicate); $**P<0.05$ (3 embryos, in triplicate). Statistical analysis was by independent two-sample *t*-test. Mean ± s.e.m. Scale bars: 60 μm in A,B; 30 μm in A′,B′; 20 μm in H,I.

Is *Neurog2* part of the combinatorial code that bestows a PC identity on cbVZ progenitors? The lack of transdifferentiation observed in genetically tagged *Neurog2* null progenitors suggests otherwise. Yet, *Neurog2* might act redundantly with other proneural genes in this context, warranting the generation and analysis of double (*Neurog1/Neurog2*) and triple (*Neurog1/Neurog2/Ascl1*) mutants to establish the roles, if any, of proneural genes in PC fate specification. Alternatively, PC identity might be conferred on multipotent *Ptf1a*$^{+}$ progenitors by other, as yet unidentified, signals, which most likely intervene before M phase of the last round of cell division. A major novel finding of this study is that Ptf1a^{+} progenitors are split into *Neurog2*$^{-}$ and *Neurog2*$^{+}$ precursors, the latter giving rise to mature PCs and DCN neurons. Our findings establish *Neurog2* as the earliest conclusive marker of this restricted subset of GABAergic lineages. Further analysis is required to determine whether *Neurog2*, by dictating cell-cycle exit, controls the binary choice between early and late GABAergic interneuron fates.

Once they arrive at the PC plate, immature PCs lose the bipolar morphology of migratory neurons and undergo complex modifications of their neurites (Miyata et al., 2010) before extending apical dendrites, from which the mature dendritic tree will arise. Thus, dendritic differentiation involves both regressive and growth changes, which follow a characteristic differentiative sequence (Ramón y Cajal, 1911; Armengol and Sotelo, 1991). Whereas the processes and mechanisms underlying the late phases of PC dendritogenesis have been extensively investigated (reviewed by Sotelo and Rossi, 2011), much less is known about the initial stages of dendrite formation and the relevant regulatory cascades that control the early steps of dendritic differentiation.

Phosphorylated Neurog2 controls apical dendrite morphology in neocortical pyramidal neurons by promoting the outgrowth of a polarized leading process during the initiation of radial migration (Hand et al., 2005). Our results indicate that *Neurog2* is required for the initial dendritic rearrangement at the end of PC migration (Armengol and Sotelo, 1991; Miyata et al., 2010). Again, both LOF and GOF results converge to implicate *Neurog2* as a key early regulator of PC dendritogenesis. *Neurog2* null PC precursors have stunted dendritic arbors. Likewise, during postnatal development, *Neurog2* null PCs exhibit hypomorphic dendrites and often fail to achieve their typical bipolar arrangement, in which the axon and a single primary dendrite emanate from opposite poles of the cell body (Sotelo, 2004; Sotelo and Rossi, 2011). Thus, *Neurog2* is important during the GC-independent phase of PC dendrite formation. The course of such early stages, however, influences the

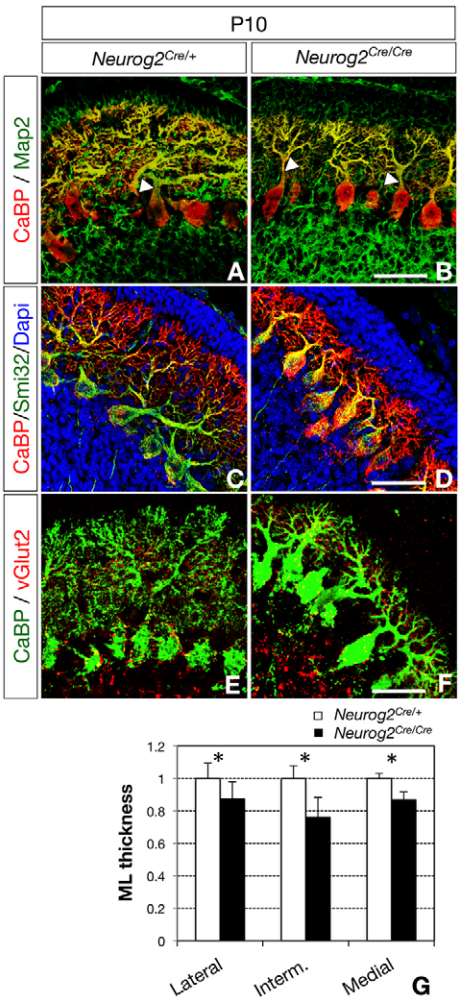

Fig. 9. Dendrite branching defects persist at P10. (**A-F**) Wild-type (A,C,E,) and *Neurog2* null mutant (B,D,F) P10 cerebella sections. (B) Null PCs co-immunostained for the dendritic markers Map2 and CaBP exhibit reduced branching and a thinned out primary dendrite (arrowheads, compare with A). (D) Immunostaining with the neurofilament marker antibody SMI32 reveals shorter and poorly branched dendrites in the *Neurog2* null mutant (compare with C). (F) Immunostaining for CaBP and the presynaptic marker Vglut2 shows that Vglut2^{+} presynaptic boutons are present normally on the dendrites of null PCs (compare with E). (**G**) Mean molecular layer (ML) thickness scored at medial, intermediate and lateral levels. *Neurog2* null cerebella exhibited reduced thickness at all levels analyzed (*P<0.02, t-test). Mean ± s.e.m. Scale bars: 40 μm.

outcome of postnatal PC dendritic arbor expansion, which is GC dependent (Sotelo, 2004). These effects of *Neurog2* become evident long after its downregulation, highlighting how instructive mechanisms that take place astride cell-cycle exit strongly affect the entire course and outcome of PC development.

Neurog2 null cerebella express reduced levels of two genes previously implicated in PC dendrite formation: *Rora*, which encodes the retinoic acid-like orphan receptor alpha, a transcription factor that plays crucial roles in PC development (Sotelo and Changeux, 1974; Herrup, 1983; Zanjani et al., 1990; Hamilton et al., 1996; Steinmayr et al., 1998); and *Sclip*, which encodes the homonymous stathmin-like phosphoprotein, a regulator of cytoskeletal dynamics (Poulain et al., 2008). *Rora* expression in fusiform PCs is crucial for dendrite regression and subsequent onset of dendritic process extension (Boukhtouche et al., 2006). Likewise, *Sclip* is implicated in the retraction of primitive processes and the formation and branching of new dendrites at early postnatal stages (Poulain et al., 2008).

Although *Rora* expression has its onset (E12.5) at the peak of *Neurog2* transcription, *Rora* clearly outlives *Neurog2*, which declines by E14.5. Neurog2, possibly in its phosphorylated form, might initiate a long-lasting and self-sustaining regulatory cascade that supports PC differentiation long after *Neurog2* downregulation. Further studies are required to assess whether Neurog2 phosphorylation is required for PC dendritogenesis.

Acknowledgements
We are grateful to Richard Hawkes for sharing unpublished results, to Gianvito Martino for his support of this project and to Cinzia Marinaro for help with viral vectors. We thank the Alembic and CFCM facilities (San Raffaele Scientific Institute) for image analysis and ES cell manipulation/blastocyst injection, respectively.

Funding
The laboratories of G.G.C. and F.R. were funded by Ataxia UK and Fondazione San Paolo. G.G.C. was also funded by Fondazione Cariplo and EU FP7 (EuroSyStem). A donation made by the Stayton family in honor of Dr Chester A. Stayton of Indianapolis, IN, USA is gratefully acknowledged. This paper is dedicated to his cherished memory. Work in the F.G. laboratory was supported by institutional funds from the UK Medical Research Council [U117570528]. Deposited in PMC for release after 6 months.

Competing interests statement
The authors declare no competing financial interests.

Supplementary material
Supplementary material available online at
http://dev.biologists.org/lookup/suppl/doi:10.1242/dev.075861/-/DC1

References

Amendola, M., Venneri, M. A., Biffi, A., Vigna, E. and Naldini, L. (2005). Coordinate dual-gene transgenesis by lentiviral vectors carrying synthetic bidirectional promoters. *Nat. Biotechnol.* **23**, 108-116.
Andersson, E., Jensen, J. B., Parmar, M., Guillemot, F. and Bjorklund, A. (2006). Development of the mesencephalic dopaminergic neuron system is compromised in the absence of neurogenin 2. *Development* **133**, 507-516.
Armengol, J. A. and Sotelo, C. (1991). Early dendritic development of Purkinje cells in the rat cerebellum. A light and electron microscopic study using axonal tracing in 'in vitro' slices. *Brain Res. Dev. Brain Res.* **64**, 95-114.
Bertrand, N., Castro, D. S. and Guillemot, F. (2002). Proneural genes and the specification of neural cell types. *Nat. Rev. Neurosci.* **3**, 517-530.
Boukhtouche, F., Janmaat, S., Vodjdani, G., Gautheron, V., Mallet, J., Dusart, I. and Mariani, J. (2006). Retinoid-related orphan receptor alpha controls the early steps of Purkinje cell dendritic differentiation. *J. Neurosci.* **26**, 1531-1538.
Britz, O., Mattar, P., Nguyen, L., Langevin, L. M., Zimmer, C., Alam, S., Guillemot, F. and Schuurmans, C. (2006). A role for proneural genes in the maturation of cortical progenitor cells. *Cereb. Cortex* **16 Suppl. 1**, i138-i151.
Carletti, B. and Rossi, F. (2008). Neurogenesis in the cerebellum. *Neuroscientist* **14**, 91-100.
Carletti, B., Grimaldi, P., Magrassi, L. and Rossi, F. (2002). Specification of cerebellar progenitors after heterotopic-heterochronic transplantation to the embryonic CNS in vivo and in vitro. *J. Neurosci.* **22**, 7132-7146.
Carletti, B., Williams, I. M., Leto, K., Nakajima, K., Magrassi, L. and Rossi, F. (2008). Time constraints and positional cues in the developing cerebellum regulate Purkinje cell placement in the cortical architecture. *Dev. Biol.* **317**, 147-160.
Casanova, E., Fehsenfeld, S., Lemberger, T., Shimshek, D. R., Sprengel, R. and Mantamadiotis, T. (2002). ER-based double iCre fusion protein allows partial recombination in forebrain. *Genesis* **34**, 208-214.
Consalez, G. G., Florio, M., Massimino, L. and Croci, L. (2011). Proneural genes and cerebellar neurogenesis in the ventricular zone and upper rhombic lip. In *Handbook of Cerebellum and Cerebellar Disorders* (ed. M. Manto, D. Gruol, J. Schmahmann, N. Koibuchi and F. Rossi). New York: Springer.
Copeland, N. G., Jenkins, N. A. and Court, D. L. (2001). Recombineering: a powerful new tool for mouse functional genomics. *Nat. Rev. Genet.* **2**, 769-779.
Corradi, A., Croci, L., Broccoli, V., Zecchini, S., Previtali, S., Wurst, W., Amadio, S., Maggi, R., Quattrini, A. and Consalez, G. G. (2003).

Hypogonadotropic hypogonadism and peripheral neuropathy in Ebf2-null mice. *Development* **130**, 401-410.
Croci, L., Chung, S. H., Masserdotti, G., Gianola, S., Bizzoca, A., Gennarini, G., Corradi, A., Rossi, F., Hawkes, R. and Consalez, G. G. (2006). A key role for the HLH transcription factor EBF2COE2,O/E-3 in Purkinje neuron migration and cerebellar cortical topography. *Development* **133**, 2719-2729.
Croci, L., Barili, V., Chia, D., Massimino, L., van Vugt, R., Masserdotti, G., Longhi, R., Rotwein, P. and Consalez, G. G. (2011). Local insulin-like growth factor I expression is essential for Purkinje neuron survival at birth. *Cell Death Differ.* **18**, 48-59.
Farah, M. H., Olson, J. M., Sucic, H. B., Hume, R. I., Tapscott, S. J. and Turner, D. L. (2000). Generation of neurons by transient expression of neural bHLH proteins in mammalian cells. *Development* **127**, 693-702.
Fode, C., Gradwohl, G., Morin, X., Dierich, A., LeMeur, M., Goridis, C. and Guillemot, F. (1998). The bHLH protein NEUROGENIN 2 is a determination factor for epibranchial placode-derived sensory neurons. *Neuron* **20**, 483-494.
Fode, C., Ma, Q., Casarosa, S., Ang, S. L., Anderson, D. J. and Guillemot, F. (2000). A role for neural determination genes in specifying the dorsoventral identity of telencephalic neurons. *Genes Dev.* **14**, 67-80.
Follenzi, A., Ailles, L. E., Bakovic, S., Geuna, M. and Naldini, L. (2000). Gene transfer by lentiviral vectors is limited by nuclear translocation and rescued by HIV-1 pol sequences. *Nat. Genet.* **25**, 217-222.
Garel, S., Marin, F., Mattei, M. G., Vesque, C., Vincent, A. and Charnay, P. (1997). Family of Ebf/Olf-1-related genes potentially involved in neuronal differentiation and regional specification in the central nervous system. *Dev. Dyn.* **210**, 191-205.
Glassmann, A., Topka, S., Wang-Eckardt, L., Anders, S., Weisheit, G., Endl, E., Zimmer, A. and Schilling, K. (2009). Basic molecular fingerprinting of immature cerebellar cortical inhibitory interneurons and their precursors. *Neuroscience* **159**, 69-82.
Goldowitz, D., Cushing, R. C., Laywell, E., D'Arcangelo, G., Sheldon, M., Sweet, H. O., Davisson, M., Steindler, D. and Curran, T. (1997). Cerebellar disorganization characteristic of reeler in scrambler mutant mice despite presence of reelin. *J. Neurosci.* **17**, 8767-8777.
Grimaldi, P., Parras, C., Guillemot, F., Rossi, F. and Wassef, M. (2009). Origins and control of the differentiation of inhibitory interneurons and glia in the cerebellum. *Dev. Biol.* **328**, 422-433.
Hamilton, B., Frankel, W., Kerrebrock, A., Hawkins, T., FitzHugh, W., Kusumi, K., Russell, L., Mueller, K., Berkel, V., Birren, B. et al. (1996). Disruption of the nuclear hormone receptor ROR-a in staggerer mice. *Nature* **379**, 736-739.
Hand, R., Bortone, D., Mattar, P., Nguyen, L., Heng, J. I., Guerrier, S., Boutt, E., Peters, E., Barnes, A. P., Parras, C. et al. (2005). Phosphorylation of Neurogenin2 specifies the migration properties and the dendritic morphology of pyramidal neurons in the neocortex. *Neuron* **48**, 45-62.
Hayashi, S. and McMahon, A. P. (2002). Efficient recombination in diverse tissues by a tamoxifen-inducible form of Cre: a tool for temporally regulated gene activation/inactivation in the mouse. *Dev. Biol.* **244**, 305-318.
Henke, R. M., Savage, T. K., Meredith, D. M., Glasgow, S. M., Hori, K., Dumas, J., MacDonald, R. J. and Johnson, J. E. (2009). Neurog2 is a direct downstream target of the Ptf1a-Rbpj transcription complex in dorsal spinal cord. *Development* **136**, 2945-2954.
Herrup, K. (1983). Role of staggerer gene in determining cell number in cerebellar cortex. I. Granule cell death is an indirect consequence of staggerer gene action. *Brain Res.* **313**, 267-274.
Hoshino, M., Nakamura, S., Mori, K., Kawauchi, T., Terao, M., Nishimura, Y. V., Fukuda, A., Fuse, T., Matsuo, N., Sone, M. et al. (2005). Ptf1a, a bHLH transcriptional gene, defines GABAergic neuronal fates in cerebellum. *Neuron* **47**, 201-213.
Hufnagel, R. B., Le, T. T., Riesenberg, A. L. and Brown, N. L. (2010). Neurog2 controls the leading edge of neurogenesis in the mammalian retina. *Dev. Biol.* **340**, 490-503.
Indra, A. K., Warot, X., Brocard, J., Bornert, J. M., Xiao, J. H., Chambon, P. and Metzger, D. (1999). Temporally-controlled site-specific mutagenesis in the basal layer of the epidermis: comparison of the recombinase activity of the tamoxifen-inducible Cre-ER(T) and Cre-ER(T2) recombinases. *Nucleic Acids Res.* **27**, 4324-4327.
Jankovski, A., Rossi, F. and Sotelo, C. (1996). Neuronal precursors in the postnatal mouse cerebellum are fully committed cells: evidence from heterochronic transplantations. *Eur. J. Neurosci.* **8**, 2308-2319.
Joyner, A. L. and Zervas, M. (2006). Genetic inducible fate mapping in mouse: establishing genetic lineages and defining genetic neuroanatomy in the nervous system. *Dev. Dyn.* **235**, 2376-2385.
Jullien, N., Goddard, I., Selmi-Ruby, S., Fina, J. L., Cremer, H. and Herman, J. P. (2008). Use of ERT2-iCre-ERT2 for conditional transgenesis. *Genesis* **46**, 193-199.
Kim, E. J., Battiste, J., Nakagawa, Y. and Johnson, J. E. (2008). Ascl1 (Mash1) lineage cells contribute to discrete cell populations in CNS architecture. *Mol. Cell. Neurosci.* **38**, 595-606.
Leto, K., Carletti, B., Williams, I. M., Magrassi, L. and Rossi, F. (2006). Different types of cerebellar GABAergic interneurons originate from a common pool of multipotent progenitor cells. *J. Neurosci.* **26**, 11682-11694.
Leto, K., Bartolini, A., Yanagawa, Y., Obata, K., Magrassi, L., Schilling, K. and Rossi, F. (2009). Laminar fate and phenotype specification of cerebellar GABAergic interneurons. *J. Neurosci.* **29**, 7079-7091.
Liu, P., Jenkins, N. A. and Copeland, N. G. (2003). A highly efficient recombineering-based method for generating conditional knockout mutations. *Genome Res.* **13**, 476-484.
Lundell, T. G., Zhou, Q. and Doughty, M. L. (2009). Neurogenin1 expression in cell lineages of the cerebellar cortex in embryonic and postnatal mice. *Dev. Dyn.* **238**, 3310-3325.
Maricich, S. M. and Herrup, K. (1999). Pax-2 expression defines a subset of GABAergic interneurons and their precursors in the developing murine cerebellum. *J. Neurobiol.* **41**, 281-294.
Mathis, L. and Nicolas, J. F. (2003). Progressive restriction of cell fates in relation to neuroepithelial cell mingling in the mouse cerebellum. *Dev. Biol.* **258**, 20-31.
Miyata, T., Kawaguchi, A., Saito, K., Kawano, M., Muto, T. and Ogawa, M. (2004). Asymmetric production of surface-dividing and non-surface-dividing cortical progenitor cells. *Development* **131**, 3133-3145.
Miyata, T., Ono, Y., Okamoto, M., Masaoka, M., Sakakibara, A., Kawaguchi, A., Hashimoto, M. and Ogawa, M. (2010). Migration, early axonogenesis, and Reelin-dependent layer-forming behavior of early/posterior-born Purkinje cells in the developing mouse lateral cerebellum. *Neural Dev.* **5**, 23.
Muzio, L., Cavasinni, F., Marinaro, C., Bergamaschi, A., Bergami, A., Porcheri, C., Cerri, F., Dina, G., Quattrini, A., Comi, G. et al. (2010). Cxcl10 enhances blood cells migration in the sub-ventricular zone of mice affected by experimental autoimmune encephalomyelitis. *Mol. Cell. Neurosci.* **43**, 268-280.
Nowakowski, R. S., Lewin, S. B. and Miller, M. W. (1989). Bromodeoxyuridine immunohistochemical determination of the lengths of the cell cycle and the DNA-synthetic phase for an anatomically defined population. *J. Neurocytol.* **18**, 311-318.
Park, T. J. and Curran, T. (2008). Crk and Crk-like play essential overlapping roles downstream of disabled-1 in the Reelin pathway. *J. Neurosci.* **28**, 13551-13562.
Pascual, M., Abasolo, I., Mingorance-Le Meur, A., Martinez, A., Del Rio, J. A., Wright, C. V., Real, F. X. and Soriano, E. (2007). Cerebellar GABAergic progenitors adopt an external granule cell-like phenotype in the absence of Ptf1a transcription factor expression. *Proc. Natl. Acad. Sci. USA* **104**, 5193-5198.
Poulain, F. E. and Sobel, A. (2007). The "SCG10-like protein" SCLIP is a novel regulator of axonal branching in hippocampal neurons, unlike SCG10. *Mol. Cell. Neurosci.* **34**, 137-146.
Poulain, F. E., Chauvin, S., Wehrle, R., Desclaux, M., Mallet, J., Vodjdani, G., Dusart, I. and Sobel, A. (2008). SCLIP is crucial for the formation and development of the Purkinje cell dendritic arbor. *J. Neurosci.* **28**, 7387-7398.
Ramón y Cajal, S. (1911). *Histologie du Système Nerveux de l'Homme et des Vertébrés*. Paris: Maloine.
Rice, D. S., Sheldon, M., D'Arcangelo, G., Nakajima, K., Goldowitz, D. and Curran, T. (1998). Disabled-1 acts downstream of Reelin in a signaling pathway that controls laminar organization in the mammalian brain. *Development* **125**, 3719-3729.
Ristanovic, D., Milosevic, N. T. and Stulic, V. (2006). Application of modified Sholl analysis to neuronal dendritic arborization of the cat spinal cord. *J. Neurosci. Methods* **158**, 212-218.
Ross, S. E., Greenberg, M. E. and Stiles, C. D. (2003). Basic helix-loop-helix factors in cortical development. *Neuron* **39**, 13-25.
Saeed, A. I., Bhagbati, N. K., Braisted, J. C., Liang, W., Sharov, V., Howe, E. A., Li, J., Thiagarajan, M., White, J. A. and Quakenbush, J. (2006). TM4 microarray software suite. *Methods Enzymol.* **411**, 134-193.
Sauer, M. E. and Walker, B. E. (1959). Radioautographic study of interkinetic nuclear migration in the neural tube. *Proc. Soc. Exp. Biol. Med.* **101**, 557-560.
Sellick, G. S., Barker, K. T., Stolte-Dijkstra, I., Fleischmann, C., Coleman, R. J., Garrett, C., Gloyn, A. L., Edghill, E. L., Hattersley, A. T., Wellauer, P. K. et al. (2004). Mutations in PTF1A cause pancreatic and cerebellar agenesis. *Nat. Genet.* **36**, 1301-1305.
Shimojo, H., Ohtsuka, T. and Kageyama, R. (2008). Oscillations in notch signaling regulate maintenance of neural progenitors. *Neuron* **58**, 52-64.
Shimshek, D. R., Kim, J., Hubner, M. R., Spergel, D. J., Buchholz, F., Casanova, E., Stewart, A. F., Seeburg, P. H. and Sprengel, R. (2002). Codon-improved Cre recombinase (iCre) expression in the mouse. *Genesis* **32**, 19-26.
Sillitoe, R. V., Gopal, N. and Joyner, A. L. (2009). Embryonic origins of ZebrinII parasagittal stripes and establishment of topographic Purkinje cell projections. *Neuroscience* **162**, 574-588.
Soriano, P. (1999). Generalized lacZ expression with the ROSA26 Cre reporter strain. *Nat. Genet.* **21**, 70-71.
Sotelo, C. (2004). Cellular and genetic regulation of the development of the cerebellar system. *Prog. Neurobiol.* **72**, 295-339.
Sotelo, C. and Changeux, J. P. (1974). Transsynaptic degeneration 'en cascade' in the cerebellar cortex of staggerer mutant mice. *Brain Res.* **67**, 519-526.

Sotelo, C. and Rossi, F. (2011). Purkinje cell migration and differentiation. In *Handbook of Cerebellum and Cerebellar Disorders* (ed. M. Manto, D. Gruol, J. Schmamann, N. Koibuchi and F. Rossi). New York: Springer.
Srinivas, S., Watanabe, T., Lin, C. S., William, C. M., Tanabe, Y., Jessell, T. M. and Costantini, F. (2001). Cre reporter strains produced by targeted insertion of EYFP and ECFP into the ROSA26 locus. *BMC Dev. Biol.* **1**, 4.
Steinmayr, M., Andre, E., Conquet, F., Rondi-Reig, L., Delhaye-Bouchaud, N., Auclair, N., Daniel, H., Crepel, F., Mariani, J., Sotelo, C. et al. (1998). staggerer phenotype in retinoid-related orphan receptor alpha-deficient mice. *Proc. Natl. Acad. Sci. USA* **95**, 3960-3965.
Sudarov, A., Turnbull, R. K., Kim, E. J., Lebel-Potter, M., Guillemot, F. and Joyner, A. L. (2011). Ascl1 genetics reveals insights into cerebellum local circuit assembly. *J. Neurosci.* **31**, 11055-11069.
Sunabori, T., Tokunaga, A., Nagai, T., Sawamoto, K., Okabe, M., Miyawaki, A., Matsuzaki, Y., Miyata, T. and Okano, H. (2008). Cell-cycle-specific nestin expression coordinates with morphological changes in embryonic cortical neural progenitors. *J. Cell Sci.* **121**, 1204-1212.
Takahashi, T., Nowakowski, R. S. and Caviness, V. S., Jr (1993). Cell cycle parameters and patterns of nuclear movement in the neocortical proliferative zone of the fetal mouse. *J. Neurosci.* **13**, 820-833.
Takahashi, T., Nowakowski, R. S. and Caviness, V. S., Jr (1995). The cell cycle of the pseudostratified ventricular epithelium of the embryonic murine cerebral wall. *J. Neurosci.* **15**, 6046-6057.
Takahashi, T., Bhide, P. G., Goto, T., Miyama, S. and Caviness, V. S., Jr (1999). Proliferative behavior of the murine cerebral wall in tissue culture: cell cycle kinetics and checkpoints. *Exp. Neurol.* **156**, 407-417.
Trommsdorff, M., Gotthardt, M., Hiesberger, T., Shelton, J., Stockinger, W., Nimpf, J., Hammer, R. E., Richardson, J. A. and Herz, J. (1999). Reeler/Disabled-like disruption of neuronal migration in knockout mice lacking the VLDL receptor and ApoE receptor 2. *Cell* **97**, 689-701.
Wechsler-Reya, R. J. and Scott, M. P. (1999). Control of neuronal precursor proliferation in the cerebellum by Sonic Hedgehog. *Neuron* **22**, 103-114.
Williams, I. M., Carletti, B., Leto, K., Magrassi, L. and Rossi, F. (2008). Cerebellar granule cells transplanted in vivo can follow physiological and unusual migratory routes to integrate into the recipient cortex. *Neurobiol. Dis.* **30**, 139-149.
Yi, S. H., Jo, A. Y., Park, C. H., Koh, H. C., Park, R. H., Suh-Kim, H., Shin, I., Lee, Y. S., Kim, J. and Lee, S. H. (2008). Mash1 and neurogenin 2 enhance survival and differentiation of neural precursor cells after transplantation to rat brains via distinct modes of action. *Mol. Ther.* **16**, 1873-1882.
Zanjani, H. S., Mariani, J. and Herrup, K. (1990). Cell loss in the inferior olive of the staggerer mutant mouse is an indirect effect of the gene. *J. Neurogenet.* **6**, 229-241.
Zhao, Y., Kwan, K.-M., Mailloux, C., Lee, W.-K., Grinberg, A., Wurst, W., Behringer, R. and Westphal, H. (2007). LIM-homeodomain proteins Lhx1 and Lhx5, and their cofactors Ldb1, control Purkinje cell differentiation in the developing cerebellum. *Proc. Natl. Acad. Sci. USA* **104**, 13182-13186.
Zordan, P., Croci, L., Hawkes, R. and Consalez, G. G. (2008). A comparative analysis of proneural gene expression in the embryonic mouse cerebellum. *Dev. Dyn.* **237**, 1726-1735.